

# Modulation of Endochondral Development of the Distal Femoral Condyle by Mechanical Loading

Sona Sundaramurthy, Jeremy J. Mao

Tissue Engineering Laboratory, University of Illinois at Chicago, 801 South Paulina Street, Chicago, Illinois 60612

Received 19 January 2005; accepted 10 June 2005

Published online 27 October 2005 in Wiley InterScience (www.interscience.wiley.com). DOI 10.1002/jor.20024

**ABSTRACT:** Although previous theoretical modeling studies have predicted that various mechanical stresses accelerate or inhibit the ossification process of the neonatal chondroepiphysis, there is a paucity of experimental data to verify these models. The present study was designed to provide experimental evidence on whether the ossification of the chondroepiphysis is modulated by mechanical loading on the distal femoral condyle explant of the neonatal (5-day-old) rabbit in organ culture. Upon aseptic dissection, the right condyle explant was immersed in and fixated to an organ culture system, and received cyclic forces at 200 mN and 1 Hz for 12 h ( $N = 8$ ) directly on its slightly convex articular surface, whereas the contralateral, left condyle explant was immersed separately in organ culture ( $N = 8$ ). Subsequently, both loaded and control explants were placed in a bioreactor rotating at 20 rpm for 72 h. In each mechanically loaded specimen, a structure reminiscent of the secondary ossification center (SOC) appeared with an average area of  $1.17 \pm 0.13 \text{ mm}^2$ , or  $15.2 \pm 8.2\%$  of the total epiphysis area. In contrast, no SOC was detected in any of the unloaded contralateral control specimens. The SOC in mechanically loaded specimens was stained intensively with fast green, whereas either the rest of the loaded epiphysis or the entire control epiphysis was stained intensely to safranin-O but lacked fast green staining. Immunolocalization revealed that the SOC of the mechanically loaded specimens expressed Runx 2 and osteopontin, both of which were absent in the unloaded control specimens. Type X collagen was expressed surrounding hypertrophic chondrocytes adjacent to the SOC, but was absent in the control specimen. Type II collagen and decorin were absent in the SOC of the loaded specimen, but were expressed throughout the rest of the loaded epiphysis and the unloaded control epiphysis. The intensity of type II collagen and decorin expression was significantly stronger among hypertrophic chondrocytes surrounding the SOC than the control. The numbers of hypertrophic chondrocytes surrounding the SOC and superior to metaphyseal bone were significantly higher in the loaded specimens than the unloaded controls. Taken together, mechanical stresses accelerate the formation of the secondary ossification center, and therefore modulate endochondral ossification. © 2005 Orthopaedic Research Society. Published by Wiley Periodicals, Inc. *J Orthop Res* 24:229–241, 2006

**Keywords:** osteoblast; chondrocyte; joint; Runx2; decorin

## INTRODUCTION

Most of the mammalian skeleton develops by endochondral ossification. A primitive cartilage model of the appendicular bone is developed during fetal morphogenesis.<sup>1–4</sup> Invasion of blood vessels at the mid-diaphysis represents the first hint of bone formation in a continuing process of the formation of the primary ossification center.<sup>4,5</sup>

In different mammalian species, the entire epiphysis of either the proximal or distal condyle is usually cartilaginous shortly before or after birth.<sup>1,4</sup> Formation of the secondary ossification center (SOC) in the center of the chondroepiphysis, shortly before, at, or after birth in various mammalian species, represents an important developmental landmark. The SOC, once fully formed, separates the chondroepiphysis into articular cartilage and growth plate cartilage.<sup>4</sup> Articular cartilage normally remains for the rest of life, whereas growth plate cartilage is replaced by bone upon the completion of longitudinal growth during puberty.<sup>4,6</sup>

Correspondence to: J.J. Mao (Telephone: 312-996-2649; Fax: 312-996-7854; E-mail: jmao2@uic.edu)

© 2005 Orthopaedic Research Society. Published by Wiley Periodicals, Inc.

As early as 1862, Hueter and Volkmann proposed that cartilage growth is regulated by mechanical forces.<sup>7</sup> Subsequent understanding of cartilage biology, however, has been enriched by cell and molecular biology studies in which cell proliferation, differentiation, and apoptosis have been related to various molecular regulatory cues.<sup>8–11</sup> However, it would have been a biased view to attribute cartilage development entirely to hereditary regulation, for mechanical stresses are critical determinants of cartilage development.<sup>1,12–14</sup> Epiphyseal cartilage was proposed to increase growth rates under both tensile and compressive loading in a juvenile chondral development model.<sup>13</sup> Experimental data have shown that cyclic forces applied to growth plates in the growing skeleton induce cellular proliferation, differentiation, matrix biosynthesis, as well as growth arrest under extreme loading.<sup>15–19</sup> However, whether chondral development is regulated by mechanical stresses in fetal or postnatal development is not well understood.

A series of finite element models have simulated loading histories of chondroepiphysis defined as discrete joint contact pressure distributions over loading cycles.<sup>12,20–22</sup> Specifically, Carter and Wong,<sup>12,23</sup> using a two-dimensional (2D) finite element model, showed that cyclic shear stresses promote endochondral ossification, whereas cyclic compressive dilatational stresses inhibit ossification. These finite element models illustrate that in the developing chondroepiphysis, the region of highest osteogenic index corresponds to the location of the secondary ossification center.<sup>21,22,24–26</sup>

Experimental data obtained by applying intermittent and continuous compressive forces to the 16-day-old metatarsal rudiment of mouse embryo in organ culture demonstrated that the mineral apposition in the primary ossification site in the center of the metatarsal cartilage rudiment is accelerated, with intermittent forces twice as effective as continuous forces.<sup>27</sup> This study suggests that mechanical stresses accelerate the formation of the primary ossification site during prenatal development.<sup>27</sup> In a follow-up study using finite element modeling, distortional strain was shown to be too small (about 2 microstrain) to have stimulated ossification of the 16-day-old embryonic metatarsal rudiment in organ culture; instead, hydrostatic pressure is responsible for the observed epiphyseal ossification.<sup>28</sup> Using a finite element model, Wong and Carter<sup>25,26</sup> postulated that the externally applied hydrostatic pressure, while purely hydrostatic at the rudiment end,

produces significant shear stresses at the cartilage/calcified cartilage interface. Accordingly, the accelerated epiphyseal osteogenesis was attributed to high shear stresses on the secondary ossification center.<sup>25,26</sup> However, there has been apparently no report of experimental data to verify whether ossification of the chondroepiphysis is induced by hydrostatic pressure or shear stresses, or both. The present study was designed to provide experimental data on whether the ossification of the chondroepiphysis is modulated by mechanical loading on the distal femoral condyle explants in neonatal (5-day-old) rabbits. Our data demonstrate *de novo* formation of a structure reminiscent of the secondary ossification center upon cyclic loading at 1 Hz and 200 mN for 12 h in an *ex vivo* organ culture system, in comparison with a lack of SOC formation in contralateral controls subjected to the same *ex vivo* culture system without exogenous mechanical loading.

## MATERIALS AND METHODS

### Animal Model and Tissue Harvesting Procedures

Eight 5-day-old New Zealand White rabbits were euthanized by intracardiac injection of 100 mg/kg Euthasol (Delmarva Laboratories, Dallas, TX). The right and left femoral condyles were dissected at the level of metaphyseal bone approximately 12 mm distal from the articular surface under aseptic conditions and immediately placed in an organ culture chamber with Dulbecco's Modified Eagle Medium (DMEM) supplemented with 10% heat inactivated fetal bovine serum (FBS), and 1% penicillin–streptomycin–L-glutamine. The overall dimension of the aseptically dissected condyle explant was 6 × 4 × 12 mm (length × width × height). The rabbit was selected as the animal model over rats or mice, because the distal femoral condyle of the neonatal rabbit probably represents the smallest size that can be manipulated *ex vivo* as in the present study. The animal procedures were approved by the institutional animal care committee.

### Exogenous Mechanical Loading

The right femoral condyle explants were rigidly fixated to the bottom of the organ culture chamber and submerged in the culture medium. Axial cyclic compressive forces at 200 mN and 1 Hz were applied to the slightly convex articular surface of the right femoral condyle explants for a total of 12 h, resulting in 43,200 cycles using a servohydraulic system (858 Mini Bionix II, MTS, Eden Prairie, MN) (Fig. 1A).<sup>18,29,30</sup> During the 12-h loading on the right femoral condyle explant, the left femoral condyle explant of the same rabbit was

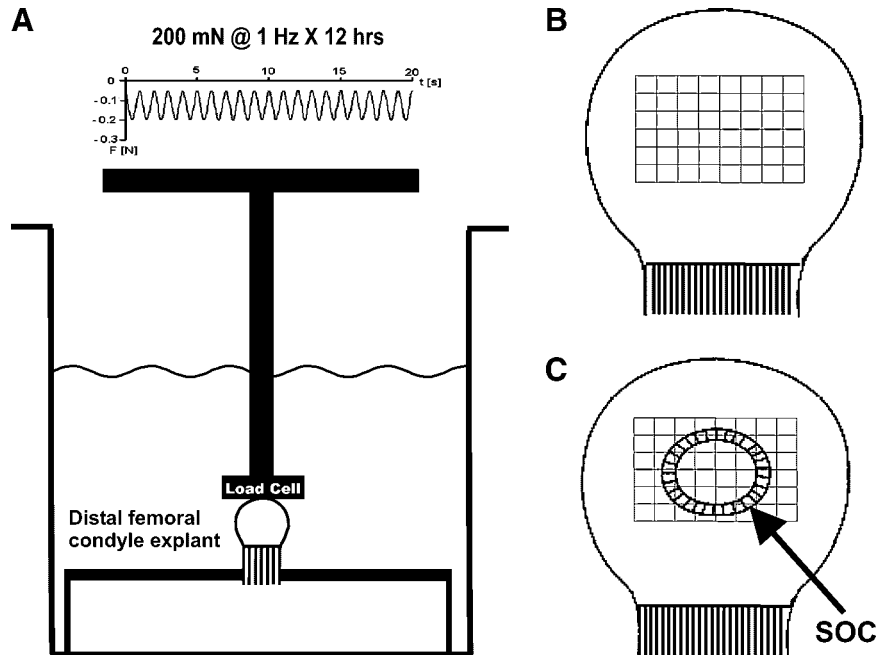


**Figure 1.** Schematic diagrams of the neonatal (5-day-old) rabbit distal femoral condyle explant in organ culture with or without exogenous cyclic (intermittent) mechanical loading, as well as methods for computer-assisted histomorphometric quantification. (A) Cyclic mechanical loading at 200 mN and 1 Hz over 12 h was applied to aseptically isolated condyle explants in organ culture. A representative force waveform was shown on the top. At 1 Hz, there was 1 cycle of loading per second. Negative values denoted compressive loading. The bony rudiment of the condyle explant was fixated rigidly. Due to the convex curvature of the articular surface of the condyle explant, both compressive and shear stresses were likely generated. The contralateral condyle explant per rabbit was immersed separately in organ culture medium, but was not subjected to exogenous cyclic loading. (B) Schematic diagram showing an unloaded control specimen with grid blocks (each  $900 \mu\text{m}^2$ ) constructed in the epiphysis. (C) Schematic diagram showing the formation of the secondary ossification center (SOC) in mechanically loaded condyle explant. The same grid blocks (each  $900 \mu\text{m}^2$ ) were constructed concentrically from the geometric center of the SOC for computer-assisted histomorphometric analysis as described in the text.

placed separately in identical organ culture medium but without any exogenous mechanical loading. Once mechanical loading of the right femoral condyle explant was completed, both the control and loaded condyle explants were placed in a rotary bioreactor. The rationale for placing control and loaded explants in bioreactor was to provide further cultivation and medium-derived nutrient supply prior to harvest.

#### Organ Culture in Rotary Bioreactor

Upon transfer to a rotary bioreactor (Synthecon, Houston, TX) containing the same organ culture medium as described above, the control and loaded femoral condyle explants were rotated at 20 rpm, and incubated for 3 days in 95% air/5%  $\text{CO}_2$  at  $37^\circ\text{C}$ . Both the control and loaded femoral condyle explants were

cultured in the same bioreactor to ensure identical hydrodynamic environment and nutrient supply. Each experiment consisted of one left femoral condyle explant (control) and one right femoral condyle explant (loaded) of the same rabbit so that the bilateral femoral condyle explants were subjected to identical conditions except for exogenous cyclic loading.

#### Tissue Processing and Histological Staining

The bioreactor-incubated femoral condyle explants were immediately fixed with 10% formalin solution overnight, followed by demineralization with 95% formic acid and 100% sodium citrate under constant perturbation using a magnetic stirrer. Upon confirmation of demineralization by X-ray, the specimens were rinsed, dehydrated in graded ethanol, treated with

xylene, and embedded in paraffin.<sup>18,29,31</sup> The entire distal femoral condyle, both mechanically loaded and controls, was first bisected along the sagittal midline under dissection microscope. A total of no less than 20 parasagittal sections from the center of the distal femoral condyle were cut sequentially at 6  $\mu\text{m}$  thickness with a microtome, and were stained with hematoxylin and eosin (H&E) and safranin-O/fast green.

### Immunohistochemistry

Sequential 6- $\mu\text{m}$  thick sections were deparaffinized, washed in PBS, rehydrated with xylene and graded ethanol, and incubated for 30 min with bovine testicular hyaluronidase (1,600 U/mL) in sodium acetate buffer (pH 5.5) with 150 mM sodium chloride. All immunohistochemical procedures were performed by Histoserv (Germantown, MD). The sections were pretreated for 20 min at 85°C with hydrogen peroxide and then with 5% bovine serum albumin (BSA) for 20 min at room temperature to block nonspecific reactions. After overnight incubation with the primary mAbs in a humidity chamber, sections were rinsed with PBS and incubated with corresponding secondary antibodies and biotin for 30 min (Table 1). Type II collagen was tested to reveal whether it is present throughout the chondroepiphysis. Type X collagen was assayed to reveal whether it is expressed in early stage of chondroepiphysis as presently studied. Runx2 and osteopontin are early- and late-stage osteogenesis markers and were assayed to determine their presence or absence in chondroepiphysis with or without mechanical loading. Microscopic sections were then incubated with streptavidin-HRP conjugate for 30 min in a humidity chamber. After washing in PBS, the double linking procedure with each secondary antibody was repeated. Slides were then stained with diaminobenzidine (DAB) solution and counterstained with Mayer's hematoxylin for 3 to 5 min. Counterstained slides were dehydrated in graded ethanol and cleared in xylene. The same procedures were performed for negative controls except for the omission of the primary mAbs.

### Computer-Assisted Histomorphometry

Standardized grids (900  $\mu\text{m}^2$ ) were constructed over the entire condyle specimens of the control (Fig. 1B) and mechanically loaded (Fig. 1C) specimens stained with safranin-O/fast green using computerized histomorphometric analysis (ImagePro Plus and Nikon Eclipse Research Microscope).<sup>18,29</sup> The number of chondrocytes with hypertrophic appearance was quantitatively assessed in the geometric center of the chondroepiphysis in control specimens or adjacent to the apparent secondary ossification center (SOC) in mechanically loaded specimens. The hypertrophic chondrocytes in each grid block were manually tagged, and automatically counted by the image analysis software. The

average total number of hypertrophic chondrocytes in nine randomly selected grid blocks per specimen was calculated for each of the control specimens, whereas the average total number of hypertrophic chondrocytes in nine grid blocks adjacent to the SOC was calculated for each of the mechanically loaded specimens. The absolute and percentage areas occupied by the SOC were measured and calculated by dividing a polygon best fit area around the SOC by a best fit of the entire cartilaginous epiphysis area. The location of the SOC within the epiphysis was measured by the vertical distance from the articular surface perpendicular to the midpoint bisecting the largest width of the SOC (c.f., Fig. 1C). The binding intensity of collagen II and decorin mAbs was expressed as DAB binding areas in six grid blocks surrounding hypertrophic chondrocytes in the periphery of the SOC and corresponding grid blocks in the control chondroepiphysis under 20 $\times$  magnification (c.f., Fig. 5A,B and E,F).

### Data Analysis and Statistics

The means and standard deviations of each quantified parameter were calculated. Upon confirmation of normal distribution, Student *t*-tests were used to determine whether mechanically loaded specimens differed significantly from control specimens. All statistical analyses were performed at an alpha level of  $p < 0.05$  using MiniTab<sup>TM</sup> software.

## RESULTS

Surgical procedures to aseptically isolate the left and right femoral condyle explants from each of a total of 8 5-day-old New Zealand White rabbits consistently yielded specimens of approximately equal dimensions. Gross examination of the isolated femoral condyle explants at the time of tissue harvest, during mechanical loading, and upon the completion of ex vivo organ culture and/or loading revealed that the condyle explants appeared intact and lacked any contamination. Exogenous cyclic compressive forces at 200 mN and 1 Hz delivered to the right femoral condyle explant fixated in an ex vivo organ culture system were consistently applied, shown as the representative force waveform generated by the load cell (Fig. 1A).

Microscopic observation of all the control, unloaded femoral condyle explants of the 5-day-old rabbits showed no appearance of the SOC ( $N=8$ ) (Fig. 2A). In contrast, formation of a structure reminiscent of the SOC appeared in each and every age- and sex-matched femoral condyle explants that received cyclic loading at

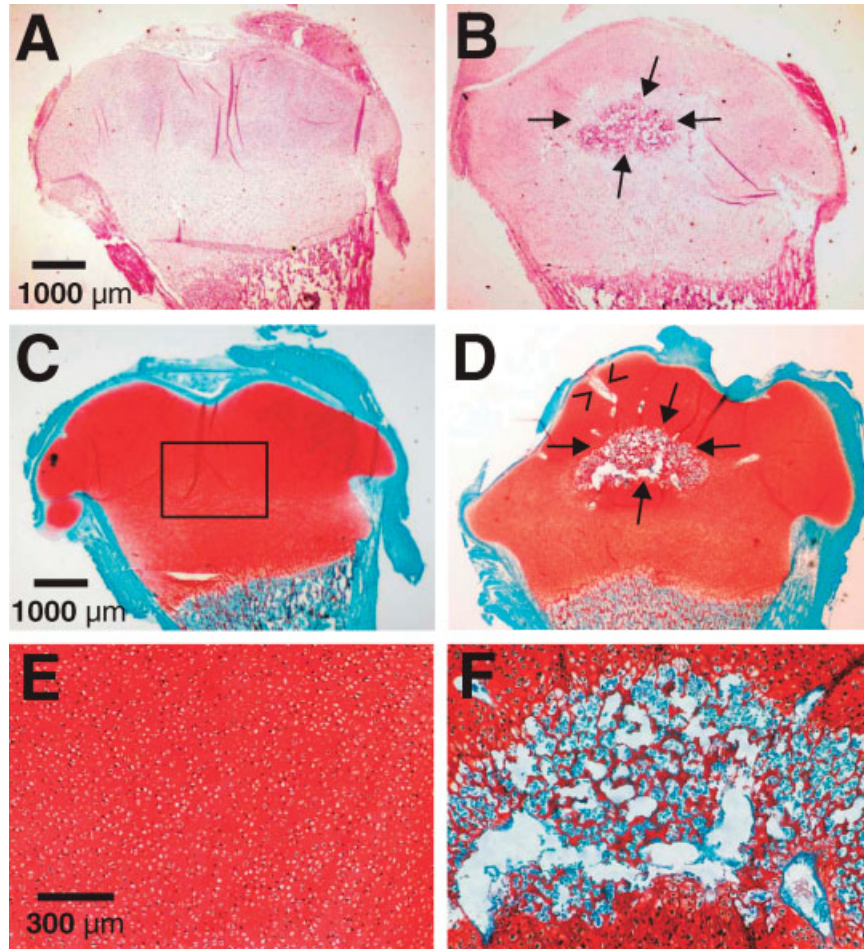


**Figure 2.** Histological examination of the control (left column) and cyclically loaded (right column) explants of the neonatal rabbit distal femoral condyles. (A) Representative H&E image of an unloaded control chondroepiphysis specimen showing that the entire epiphysis was cartilaginous and the absence of the secondary ossification center (SOC). (B) Representative H&E image of a mechanically loaded specimen showing the presence of SOC between arrows. (C) Representative safranin-O/fast green counterstaining of an unloaded control chondroepiphysis specimen showing that the entire epiphysis was stained positively to safranin-O, indicating the presence of abundant aggrecan molecules. The control chondroepiphysis lacked fast green staining except in its perichondrium. (D) Representative safranin-O/fast green counterstaining of a cyclically loaded specimen showing that formation of the SOC counterstained with fast green (between arrows). (E) Higher magnification of (C) showing chondrocytelike cells residing in the safranin-O positive matrix from the rectangle in (C). The chondrocytelike cells lacked the morphological appearance of hypertrophy, and resembled proliferating chondrocytes, instead of hypertrophic chondrocytes. (F) Higher magnification of the SOC in (D) showing safranin-O positive areas in the periphery and sparsely in the SOC but surrounded by abundant fast green positive structures that resemble bone trabeculae.

1 Hz and 200 mN ( $N=8$ ) (between arrows in Fig. 2B). Safranin-O/fast green counterstaining revealed that the epiphysis of the unloaded control femoral condyle explant was entirely cartilaginous (Fig. 2C). Formation of the SOC was confirmed by safranin-O/fast green counterstain in all mechani-

cally loaded explants (between arrows in Fig. 2D). High magnification showed chondrocytelike cells throughout the control, unloaded left femoral condyle explants (Fig. 2E). In comparison, few chondrocytes were present in the SOC of mechanically loaded condyle explants, although the SOC

contained cells that were labeled positive to fast green (Fig. 2F). The structures labeled by fast green in the center of the SOC were reminiscent of bone trabeculae (Fig. 2F). Some of the chondrocytes surrounding the SOC appeared hypertrophic (Fig. 2F), in comparison with the appearance of proliferating chondrocytes throughout the unloaded control chondroepiphysis (Fig. 2E). Mechanically loaded condyle explants contained canal-like structures (c.f., Fig. 2D), in comparison with few canal-like structures in unloaded control specimens (Fig. 2C). A higher magnification of the canal-like structure in Figure 2D (between two arrowheads) was shown in Figure 3A. In this case, the canal-like structure contained cellular components and appeared to communicate with the perichondrium (Fig. 3A). The average number of canal-like structures in mechanically loaded specimens ( $N=8$ ) was significantly higher than unloaded control specimens ( $N=8$ ) ( $p < 0.001$ ) (Fig. 3B).

Immunohistochemical labeling of deparaffinized specimens with monoclonal antibodies (mAb) against Runx 2 (CBFA1) and osteopontin, which were early and late osteogenesis markers, revealed differences between control and cyclically loaded specimens. There was a general lack of mAb labeling of Runx 2 in the unloaded control chondroepiphysis of the 5-day-old femoral condyle explant (Fig. 4A). In contrast, intense Runx 2 mAb staining was present in the age- and sex-matched femoral condyle explant that received cyclic load-

ing at 1 Hz and 200 mN (Fig. 4B). Runx 2 mAb was immunolocalized only to the SOC in the mechanically loaded specimen, but not in the rest of the epiphysis (Fig. 4B). Similarly, osteopontin was intensely immunolocalized to the SOC (Fig. 4D), but not in either the rest of mechanically loaded epiphysis or in the unloaded control chondroepiphysis (Fig. 4C).

Control and cyclically loaded specimens also differed in their immunostaining of cartilaginous markers including type II collagen, type X collagen, and decorin. Type II collagen, the major structural protein of cartilage, was present throughout the chondroepiphysis of the unloaded control condyle explant (Fig. 5A). In contrast, although type II collagen was expressed in the epiphysis, the mechanically loaded specimen generally lacked type II collagen immunostaining in the SOC (Fig. 5B). There was a lack of immunostaining with type X collagen, a specific marker for chondrocyte hypertrophy in the unloaded control specimen (Fig. 5C), indicating that the abundant chondrocytes seen in the unloaded control specimen in Figure 2E are likely proliferating chondrocytes without undergoing hypertrophy. In comparison, sparse areas of type X collagen immunolocalization were present in the periphery of the SOC of the mechanically loaded specimen (Fig. 5D). Decorin, a small proteoglycan that interacts with type II collagen fibrils, was present throughout the chondroepiphysis of the unloaded control condyle explant (Fig. 5E). In contrast, the

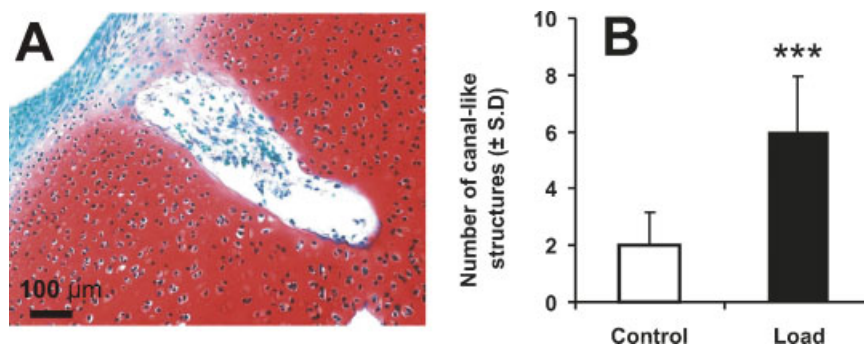


**Figure 3.** A representative canal-like structure in mechanically loaded rabbit neonatal condyle explant and quantification of canal-like structures in both control and loaded specimens. (A) A representative, higher magnification canal-like structure that was shown in Figure 2D between arrowheads. This canal-like structure in the mechanically loaded specimen may communicate with the perichondrium, as shown in Figure 3A. (B) The average number of canal-like structures in mechanically loaded specimens ( $N=8$ ) was significantly higher than unloaded control specimens ( $N=8$ ).  $***p < 0.001$ . [Color scheme can be viewed in the online issue, which is available at <http://www.interscience.wiley.com>]

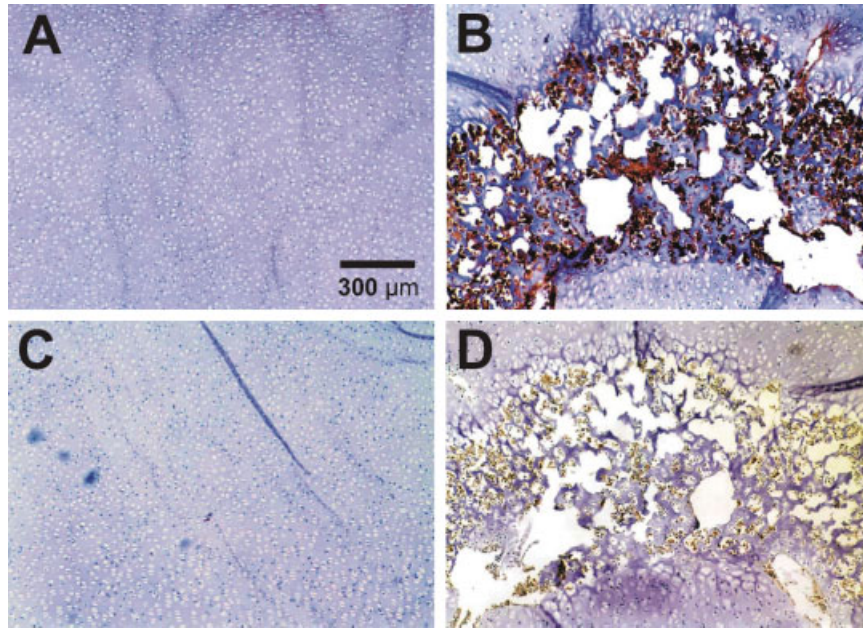


**Figure 4.** Representative immunolocalization of Runx 2 and osteopontin in both control (left column) and loaded (right column) neonatal rabbit distal femoral condyle explants. (A) Control explant showing a general lack of Runx 2 expression. (B) The cyclically loaded explant showing positive Runx 2 expression within the secondary ossification center (SOC). (C) Control explant showing a general lack of osteopontin expression. (D) The cyclically loaded explant showing positive osteopontin expression within the SOC. [Color scheme can be viewed in the online issue, which is available at <http://www.interscience.wiley.com>]

SOC generally lacked decorin immunostaining, despite the general presence of decorin immunolocalized to the epiphysis of the mechanically loaded specimen (Fig. 5F).

Quantification of several parameters of the microscopic images revealed interesting characteristics of the control and mechanically loaded neonatal femoral condyle explants by computerized image analysis. The average area occupied by the SOC in cyclically loaded specimens was  $1.17 \pm 0.13 \text{ mm}^2$  (mean  $\pm$  SD), or  $15.2 \pm 8.2\%$  of the total epiphysis area ( $N=8$ ) (Fig. 6A), in comparison with the absence of the SOC in all unloaded control specimens ( $N=8$ ). The superior border of the SOC in all mechanically loaded samples was approximately in the upper third of the epiphysis, coinciding with the superior third distance of the entire epiphysis (Fig. 6B). By using standardized grids ( $900 \text{ } \mu\text{m}^2$ ) constructed over the femoral condyle explant stained with safranin-O/fast green as in Figure 2C,D, hypertrophic chondrocytes were counted with their numbers averaged from nine randomly selected grid blocks sepa-

rately for the control and mechanically loaded specimens. The average number of hypertrophic chondrocytes in nine grid blocks adjacent to the SOC in the cyclically loaded specimen at  $29 \pm 6/900 \text{ } \mu\text{m}^2$  was significantly greater than the average number of hypertrophic chondrocytes in nine randomly selected grid blocks for the unloaded control specimens at  $12 \pm 2/900 \text{ } \mu\text{m}^2$  ( $p < 0.001$ ) (Fig. 6C). Although the nine grid blocks for the control specimen were randomly selected throughout the entire chondroepiphysis, the small variance in the number of counted chondrocytes ( $12 \pm 2/900 \text{ } \mu\text{m}^2$ ) provided validation for the random selection of grid blocks in control specimens. Similarly, the average number of hypertrophic chondrocytes superior to metaphyseal bone in nine grid blocks in the cyclically loaded specimens was  $56 \pm 5/900 \text{ } \mu\text{m}^2$ , significantly higher than the average number of hypertrophic chondrocytes superior to metaphyseal bone in nine grid blocks of unloaded control specimens at  $41 \pm 6/900 \text{ } \mu\text{m}^2$  ( $p < 0.001$ ) (Fig. 6D). The intensity of mAb staining also showed significant differences between

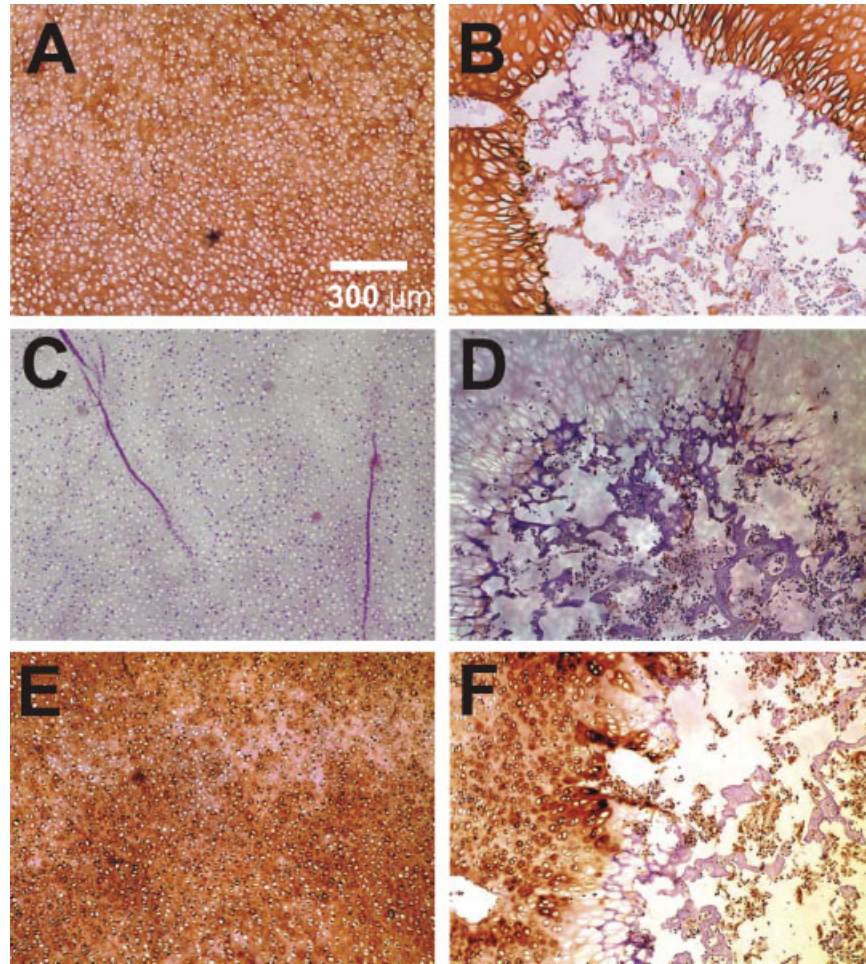


**Figure 5.** Representative immunolocalization of type II collagen, type X collagen, and decorin in both control (left column) and loaded (right column) neonatal rabbit distal femoral condyle explants. (A) Control explant showing type II collagen expression thoroughly in the chondroepiphysis. (B) The cyclically loaded explant showing little type II collagen within the secondary ossification center (SOC). (C) Control explant showing a general lack of type X collagen expression, which is a chondrocyte hypertrophy marker. (D) The cyclically loaded condyle explant showing sparse type X collagen expression within the SOC. (E) Control explant showing decorin expression thoroughly in the chondroepiphysis. (F) The cyclically loaded explant showing positive decorin expression in chondroepiphysis, but only sparse decorin expression within the secondary ossification center (SOC). [Color scheme can be viewed in the online issue, which is available at <http://www.interscience.wiley.com>]

control and mechanically loaded specimens. The average intensity of decorin mAb staining for the cyclically loaded specimen was  $6.7 \pm 0.3/900 \mu\text{m}^2$ , significantly higher than the corresponding control specimen at  $3.97 \pm 0.14/900 \mu\text{m}^2$  (Fig. 6E). Similarly, the average staining intensity of collagen II collagen mAb for the cyclically loaded specimen was  $20.5 \pm 1.5/900 \mu\text{m}^2$ , significantly higher than the unloaded control specimen at  $5.6 \pm 0.4/900 \mu\text{m}^2$  (Fig. 6F).

## DISCUSSION

The mechanically induced secondary ossification center bears close morphological resemblance to the natural secondary ossification center in neonatal rabbit femur.<sup>4</sup> The present findings provide experimental evidence that the formation of the secondary ossification center in the neonatal (5-day-old) rabbit chondroepiphysis is accelerated by intermittent contact loading on the distal

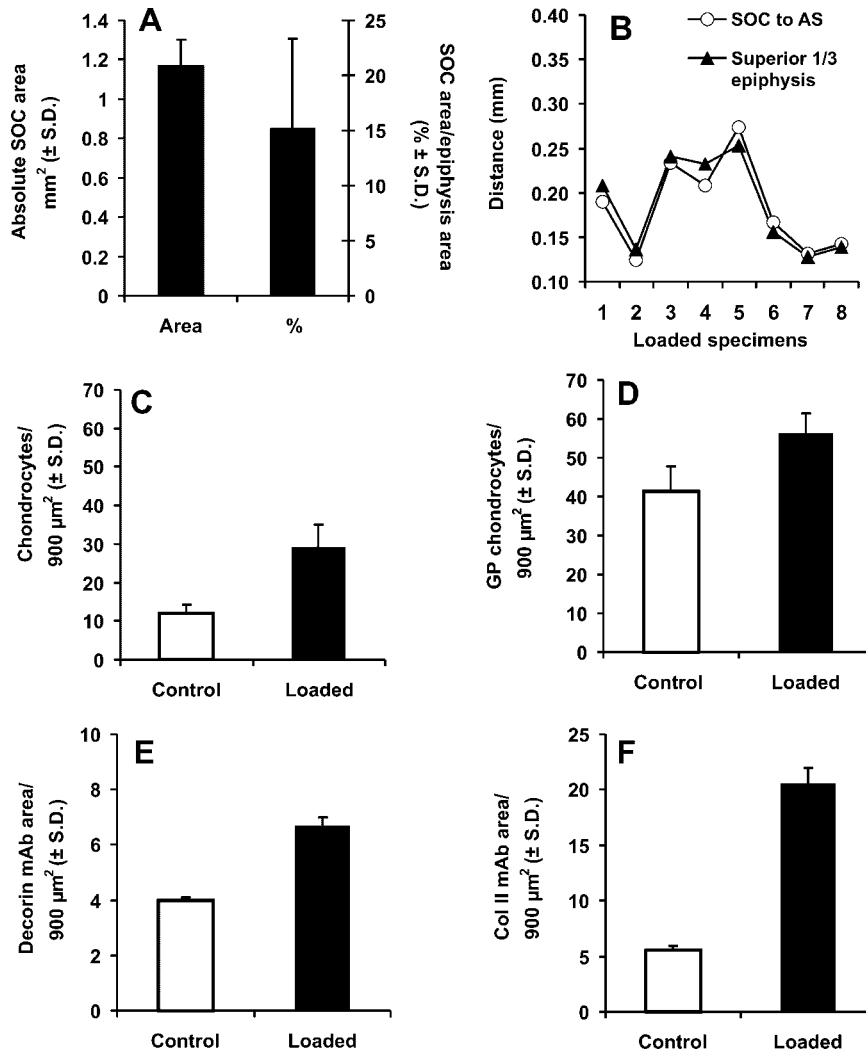


**Figure 6.** Computer-assisted histomorphometric quantification. (A) The area occupied by the secondary ossification center (SOC) in mechanically loaded specimens ( $N = 8$ ) was significantly higher than the unloaded control specimens ( $N = 8$ ). The average area occupied by the SOC divided by the total area of chondroepiphysis in cyclically loaded explants ( $N = 8$ ) was significantly higher than control explants ( $N = 8$ ). (B) The location of the SOC within the epiphysis was measured by the vertical distance from the articular surface perpendicular to the midpoint bisecting the largest width of the SOC. AS, articular surface. (C) The average number of hypertrophic chondrocyte-like cells surrounding the SOC in cyclically loaded explants ( $N = 8$ ) was significantly greater than the corresponding region of the control explants ( $N = 8$ ) ( $p < 0.001$ ). (D) The average number of hypertrophic chondrocytelike cells superior to the future growth plate (c.f. Fig. 2) in cyclically loaded explants ( $N = 8$ ) was significantly greater than corresponding regions of the control explants ( $N = 8$ ) ( $p < 0.001$ ). (E) The intensity of decorin monoclonal antibody (mAb) staining in hypertrophic chondrocytelike cells surrounding the SOC in cyclically loaded explants ( $N = 8$ ) was significantly greater than corresponding regions of the control explants ( $N = 8$ ) ( $p < 0.01$ ). (F) The intensity of type II collagen antibody staining in hypertrophic chondrocytelike cells surrounding the SOC in cyclically loaded explants ( $N = 8$ ) was significantly greater than corresponding regions of the control explants ( $N = 8$ ) ( $p < 0.01$ ). \*\* $p < 0.01$ ; \*\*\* $p < 0.001$ .

femoral condyle explant *in vitro* in organ culture, in comparison with a lack of formation of the secondary ossification center in the contralateral control condyle explants. The present intermittent loading system induces contact pressure on the 5-day-old rabbit distal femoral condyle explants that have a slight convex curvature near its geometric center on the articular surface. Thus, both compressive stresses and shear stresses are likely generated within the chondroepiphysis, providing preliminary support of some of the finite element model predictions.<sup>12,20–22</sup> Although the present intermittent loading system does not generate hydrostatic pressure on the gas phase of the organ culture medium due to immersion of the loading piston within the organ culture medium, these data may not be considered as experimental evidence to rule out the possibility that hydrostatic pressure may also accelerate the ossification of the chondroepiphysis.<sup>28</sup> In another finite element model, hydrostatic pressure has been found to generate shear stresses at the cartilage/calcified cartilage interface, although pure hydrostatic pressure is detected at the bone end of the chondroepiphysis.<sup>25,26</sup> Furthermore, simulated four-point bending applied to unmineralized and mineralized embryonic mouse ribs at 16 and 17 days of gestational age in a finite element model increases their Young's moduli by two orders of magnitude within 1 day, implicating that the presently used direct loading of chondroepiphysis may result in substantial stress shielding for hypertrophic chondrocytes.<sup>32</sup> Enhanced <sup>45</sup>Ca and <sup>32</sup>P incorporation in the metatarsal condyle upon both intermittent and continuous compressive hydrostatic pressure in Klein-Nulend and colleagues<sup>27</sup> warrants additional studies to verify whether the formation of the secondary ossification center is accelerated also by hydrostatic pressure, perhaps at different magnitude and durations.

The formation of the apparent secondary ossification center is evidenced by morphological changes in the chondroepiphysis in the 5-day-old distal femoral condyle explant, the presence of Runx 2 and osteopontin in the SOC, and strong expression of type II collagen and decorin in the chondroepiphysis in both the loaded and control specimens, but a general lack of their expressions in the SOC. Decorin interacts with the core protein of type II collagen fibrils and is likely involved in regulating chondrocyte proliferation.<sup>33</sup> Recently, decorin has been shown to be upregulated by mechanical stresses applied to several connective

tissues such as the tendon, annulus fibrosus, and the neonatal growth plate.<sup>19,34,35,46</sup> Thus, it is probable that decorin, as a small proteoglycan present in multiple connective tissues, is responsive to mechanical stresses, and in turn may regulate both type I and type II collagen fibrils. Indeed, increases in decorin and type II collagen adjacent to the SOC in Figure 5 can probably be attributed to the biphasic environment of cells surrounding the SOC.<sup>1</sup> Type X collagen is a marker for chondrocyte hypertrophy as seen in the later stages of epiphyseal development,<sup>36,37</sup> but was virtually absent in the control chondroepiphysis of the present 5-day-old distal femoral condyle, suggesting that the chondrocytes in the control chondroepiphysis are proliferating chondrocytes instead of hypertrophic chondrocytes. In contrast, the expression of type X collagen among hypertrophic chondrocytes adjacent to the SOC in mechanically loaded specimens suggests that mechanical stresses accelerate cartilage maturation. Furthermore, accelerated cartilage maturation by mechanical stresses is evidenced by significantly more hypertrophic chondrocytes in mechanically loaded condyle specimens both adjacent to the SOC and superior to metaphyseal bone.

The appearance of the secondary ossification center in the present *ex vivo* organ culture system under cyclic loading warrants speculations as to the mechanisms of its formation. During natural formation of the SOC, vascular invasion from the perichondrium is considered to take place by invagination and then canals in epiphyseal cartilage, leading to further mineralization of the chondroepiphysis.<sup>38–42</sup> However, angiogenesis should have been arrested after 12 h in either the presently loaded explants or control explants in organ culture medium, followed by 3 days of additional culture in a rotary bioreactor. It is unlikely that angiogenesis, at least in the sense of *in vivo* angiogenesis, has played any significant role in the formation of the SOC in the present *ex vivo* organ culture system. On the other hand, it is possible that these canals are early endothelial structures and should be assayed for endothelial markers such as CD31, CD133, etc.

An alternative explanation for the mechanically induced formation of the SOC is that the cells in the center of the chondroepiphysis switched lineages from chondrocytes to osteoblastlike cells under cyclic loading. Although the epiphysis is conventionally considered to be cartilaginous prior to the formation of the secondary ossification center, some of the cells in the chondroepiphysis are likely

mesenchymal stem cells or chondroprogenitor cells, which upon appropriate mechanical loading, may readily differentiate into osteoblasts. Mechanically induced perfusion and fluid flow in a biphasic environment may favor phenotypic differentiation of chondrogenic cells.<sup>1</sup> Deformation of chondrocytes and extracellular matrix components in the biphasic environment has profound effects on cartilage's metabolism.<sup>1</sup> Recent tissue-engineering experiments have demonstrated a high level of plasticity of differentiation of mesenchymal stem cells into osteoblasts.<sup>43–45</sup> It is then probable that in this case, the canal-like structures may radiate from the secondary ossification center outwards toward the perichondrium. Further experiments using serial observation/reconstruction methods and/or analysis of the expression of angiogenic and other matrix markers are necessary to determine the mechanisms of mechanically induced SOC formation *ex vivo*.

Additional studies are necessary to address the following issues. The loading frequency of 1 Hz and amplitude at 200 mN has been estimated to simulate the frequency of physiological activities such as gait in neonatal rabbits. Assuming that the presently adopted mechanical parameters resemble those in function to a certain degree, they might have represented condensation of physiological activities over a period of time to 12 h in the present *ex vivo* organ culture system. However, it is probable that 12 h of exogenous cyclic loading were excessive for inducing the observed acceleration in the formation of the secondary ossification center. The possibility that the SOC is inducible by fewer cycles of intermittent loading should be investigated. Also, additional studies are necessary to determine whether the SOC in mechanically loaded specimens was formed upon the completion of the 12-h cyclic loading or upon the completion of 3 additional days of *ex vivo* organ culture. The effects of cell culture ingredients on the appearance of SOC should be further investigated. Given that the presently used force magnitude of 200 mN induces the formation of the SOC in each and every mechanically loaded specimen, and the absence of the SOC in contralateral unloaded controls, it is likely that the threshold of mechanical forces for inducing the accelerated formation of the SOC is less than 200 mN, and should be investigated. Several other biomechanical issues should also be addressed, such as the effects of a duty cycle, for example, 3 h on, 3 h off.

Within the constraints of the present study, we demonstrate that milliNewton contact loading of the neonatal distal femoral condyle explant with a cyclic force induces the acceleration in the formation of the secondary ossification center in organ culture. Morphologically, the mechanically induced secondary ossification center resembles those formed in nature.<sup>4</sup> Immunohistochemically, the mechanically induced secondary ossification center expresses bone markers and lacks cartilage markers. It is evident that mechanical stresses indeed modulate chondral development, although the exact nature of the mechanical stimuli warrants further investigations.

## ACKNOWLEDGMENTS

The experimental work described in this manuscript was derived from the Master of Science thesis research by Sona Sundaramurthy. We thank Drs. Michael Cho and D. Rick Sumner for serving on the thesis committee, and their valuable input on improving the quality of the thesis. We are grateful to Dr. Gwendolen Reilly for her valuable comments on a thesis draft and for her assistance with real-time polymerase chain reaction procedures. We thank Aurora Lopez for general technical assistance. This research was supported in part by a Biomedical Engineering Research Grant from the Whitaker Foundation (RG-01-0075), and by NIH grants DE13964, DE15391, and EB02332.

## REFERENCES

1. Mow VC, Ateshian GA, Spilker RL. 1993. Biomechanics of diarthrodial joints: a review of twenty years of progress. *J Biomech Eng* 115:460–467.
2. Ogden JA, McCarthy SM. 1983. Radiology of postnatal skeletal development. VIII. Distal tibia and fibula. *Skeletal Radiol* 10:209–220.
3. Panattoni GL, D'Amelio P, Di Stefano M, et al. 2000. Ossification centers of human femur. *Calcif Tissue Int* 66:255–258.
4. Rivas R, Shapiro F. 2002. Structural stages in the development of the long bones and epiphyses. *J Bone Joint Surg* 84A:85–100.
5. Connolly SA, Jaramillo D, Hong JK, et al. 2004. Skeletal development in fetal pig specimens: MR imaging of femur with histologic comparison. *Radiology* (in press).
6. Buckwalter JA. 2000. Advancing the science and art of orthopaedics. Lessons from history. *J Bone Joint Surg Am* 82:1782–1803.
7. Carter DR, Beaupre GS. 2001. Skeletal function and form. New York: Cambridge University Press; pp. 40–51.

8. Pacifici M. 1995. Tenascin-C and the development of articular cartilage. *Matrix Biol* 14:689–698.
9. de Crombrughe B, Lefebvre V, Nakashima K. 2001. Regulatory mechanisms in the pathways of cartilage and bone formation. *Curr Opin Cell Biol* 13:721–727.
10. Loeser RF. 2002. Integrins and cell signaling in chondrocytes. *Biorheology* 39:119–124.
11. Shum L, Nuckolls G. 2002. The life cycle of chondrocytes in the developing skeleton. *Arthritis Res* 4:94–106.
12. Carter DR, Wong M. 1988. Mechanical stresses and endochondral ossification in the chondroepiphysis. *J Orthop Res* 6:148–154.
13. Frost HM. 1990. Skeletal structural adaptations to mechanical usage (SATMU): 3. The hyaline cartilage modeling problem. *Anat Rec* 226:423–432.
14. Mao JJ, Nah H-D. 2004. Growth and development: hereditary and mechanical modulations. *Am J Orthod Dentofac Orthop* 25:676–689.
15. Ohashi N, Robling AG, Burr DB, et al. 2002. The effects of dynamic axial loading on the rat growth plate. *J Bone Miner Res* 17:284–292.
16. Stokes IA, Mente PL, Iatridis JC, et al. 2002. Enlargement of growth plate chondrocytes modulated by sustained mechanical loading. *J Bone Joint Surg* 84A:1842–1848.
17. Robling AG, Duijvelaar KM, Geevers JV, et al. 2001. Modulation of appositional and longitudinal bone growth in the rat ulna by applied static and dynamic force. *Bone* 29:105–113.
18. Wang X, Mao JJ. 2002. Accelerated chondrogenesis of the rabbit cranial base growth plate upon oscillatory mechanical stimuli. *J Bone Miner Res* 17:457–462.
19. Mao JJ. 2005. Calvarial development: cells and mechanics. *Curr Opin Orthop* 16:331–337.
20. Carter DR, Wong M, Orr TE. 1991. Musculoskeletal ontogeny, phylogeny, and functional adaptation. *J Biomech* 24(Suppl 1):3–16.
21. Stevens SS, Beaupre GS, Carter DR. 1999. Computer model of endochondral growth and ossification in long bones: biological and mechanobiological influences. *J Orthop Res* 17:646–653.
22. Carter DR, Wong M. 2003. Modelling cartilage mechanobiology. *Philos Trans R Soc Lond B Biol Sci* 29:1461–1471.
23. Carter DR, Wong M. 1988. The role of mechanical loading histories in the development of diarthrodial joints. *J Orthop Res* 6:804–816.
24. Beaupre GS, Stevens SS, Carter DR. 2000. Mechanobiology in the development, maintenance and degeneration of articular cartilage. *J Rehabil Res Dev* 37:145–151.
25. Wong M, Carter DR. 1990. A theoretical model of endochondral ossification and bone architectural construction in long bone ontogeny. *Ant Embryol* 181:523–532.
26. Wong M, Carter DR. 1990. Theoretical stress analysis of organ culture osteogenesis. *Bone* 11:127–131.
27. Klein-Nulend J, Veldhuijzen JP, Burger EH. 1986. Increased calcification of growth plate cartilage as a result of compressive force in vitro. *Arthritis Rheum* 29:1002–1009.
28. Tanck E, Van Driel WD, Hagen JW, et al. 1999. Why does intermittent hydrostatic pressure enhance the mineralization process in fetal cartilage? *J Biomech* 32:153–161.
29. Kopher RA, Mao JJ. 2003. Sutural growth modulated by the oscillatory component of micromechanical strain. *J Bone Miner Res* 18:521–528.
30. Mao JJ, Wang X, Kopher RA, et al. 2003. Strain induced osteogenesis in the cranial suture upon controlled delivery of low-frequency cyclic forces. *Front Biosci* 8:a10–a17.
31. Mao JJ, Rahemtulla F, Scott PG. 1998. Proteoglycan expression in articular tissues of the rat temporomandibular joint in response to bite raise. *J Dent Res* 77:1520–1528.
32. Tanck E, Van Donkelaar CC, Jepsen KJ, et al. 2004. The mechanical consequences of mineralization in embryonic bone. *Bone* 35:186–190.
33. Mochida Y, Duarte WR, Tanzawa H, et al. 2003. Decorin modulates matrix mineralization in vitro. *Biochem Biophys Res Commun* 305:6–9.
34. Elliott DM, Robinson PS, Gimbel JA, et al. 2003. Effect of altered matrix proteins on quasilinear viscoelastic properties in transgenic mouse tail tendons. *Ann Biomed Eng* 31:599–605.
35. Wang YN, Sanders JE. 2003. How does skin adapt to repetitive mechanical stress to become load tolerant? *Medical Hypotheses* 61:29–35.
36. Schmid TM, Linsenmayer TF. 1985. Developmental acquisition of type X collagen in the embryonic chick tibiotarsus. *Dev Biol* 107:373–381.
37. Gibson G, Lin DL, Francki K, et al. 1996. Type X collagen is colocalized with a proteoglycan epitope to form distinct morphological structures in bovine growth cartilage. *Bone* 19:307–315.
38. Floyd WE 3rd, Zaleske DJ, Schiller AL, et al. 1987. Vascular events associated with the appearance of the secondary center of ossification in the murine distal femoral epiphysis. *J Bone Joint Surg Am* 69:185–190.
39. Delgado-Baeza E, Gimenez-Ribotta M, Miralles-Flores C, et al. 1991. Morphogenesis of cartilage canals: experimental approach in the rat tibia. *Acta Anat (Basel)* 142:132–137.
40. Ganey TM, Love SM, Ogden JA. 1992. Development of vascularization in the chondroepiphysis of the rabbit. *J Orthop Res* 10:496–510.
41. Ganey TM, Ogden JA, Sasse J, et al. 1995. Basement membrane composition of cartilage canals during development and ossification of the epiphysis. *Anat Rec* 241:425–437.

42. Brown RA, Blunn GW, Salisbury JR, et al. 1993. Two patterns of calcification in primary (physeal) and secondary (epiphyseal) growth cartilage. *Clin Orthop* 294:318–324.
43. Alhadlaq A, Mao JJ, Hong L, et al. 2004. Adult stem cell driven genesis of human-shaped articular condyle. *Ann Biomed Eng* 32:911–923.
44. Alhadlaq A, Mao JJ. 2003. Tissue-engineered neogenesis of human-shaped mandibular condyle from rat mesenchymal stem cells. *J Dent Res* 82: 950–955.
45. Caplan AI. 2000. Mesenchymal stem cells and gene therapy. *Clin Orthop* 379(Suppl):S67–S70.